Beyond mean-field ground-state energies and correlation properties of a trapped Bose-Einstein condensate

S. A. Sofianos,[1] T. K. Das,[1,2] B. Chakrabarti,[3] M. L. Lekala,[1] R. M. Adam,[1,*] and G. J. Rampho[1]

[1]*Department of Physics, University of South Africa, P.O. Box 392, Pretoria 0003, South Africa*

[2]*Department of Physics, University of Calcutta, 92 A.P.C. Road, Kolkata 700009, India*

[3]*Department of Physics, University of Kalyani, Kalyani 741235, India*

(Received 19 May 2012; revised manuscript received 15 October 2012; published 9 January 2013)

A two-body correlated basis set is used to develop a many-body theory which is valid for any number of bosons in the trap. The formalism incorporates the van der Waals interaction and two-body correlations in an exact way. The theory has successfully been applied to Bose-Einstein condensates—dilute weakly interacting and also dilute but having a large scattering length. Even in the extreme dilute condition, we observe the breakdown of the shape-independent approximation and the interatomic correlation plays an important role in the large particle-number limit. This correlated many-body calculation can handle, within the two-body correlation approximation, the entire range of atom number of experimentally achieved condensates. Next we successfully push the basis function for large scattering lengths where the mean-field results are manifestly bad. The sharp increase in correlation energy clearly shows the beyond-mean-field effect. We also calculate one-particle densities for various scattering lengths and particle numbers. Our many-body calculation exhibits the finite-size effect in the one-body density.

DOI: 10.1103/PhysRevA.87.013608 PACS number(s): 03.75.Hh, 03.65.Ge

I. INTRODUCTION

Since the first experimental observation of Bose-Einstein condensation (BEC) in trapped ultracold atomic vapors, there has been a renewed interest in a theoretical description of the phenomenon [1]. In dilute Bose gases at low temperatures, the effective atomic interactions have a range much smaller than the interparticle separation. The number of condensed atoms (A) in the experimental trap varies from a few to several million. The most commonly used approach to describe such a dilute gas of a large number of atoms is the mean-field theory [2]. At $T = 0$, as the interatomic interaction is described by the zero-range contact potential, the mean-field equation takes the form of the time-independent Gross-Pitaveskii (GP) equation [2]. In the GP mean-field description of the condensate properties, the atomic interaction is solely determined by the mean-field potential which is proportional to the s-wave scattering length (a_s). Despite the success of the GP equation in the weakly interacting regime, the shape-independent approximation is one of the weak points of the GP equation. It also does not include particle-particle correlation. In contrast, a full quantum many-body calculation by the essentially exact diffusion Monte Carlo (DMC) method keeps all many-body correlations [3–5]. This method has already been applied to describe the ground-state properties of dilute BEC [3] for A up to 100 particles in the trap and the numerical results confirm the need for quantum corrections not included in the mean-field equation. However, due to computational difficulties, the extension of DMC to the entire range of atom number of experimentally achieved BEC is not possible. Thus the key role played by the actual finite-range interatomic potential and the effect of particle-particle correlation for a large A limit needs additional study.

The main motivation of our work is to employ a many-body method which can treat quite a large number of atoms ($A \simeq 10^6$) in the trap, take the two-body correlations among bosons in the dilute regime into account, and use a realistic (*van der Waals*) potential. At $T = 0$, as the Bose gas is extremely dilute, only two-body collisions become important and one can safely ignore the three- and higher-body collisions. Thus the interatomic correlation in the two-body level and the use of a two-body correlated basis function in the description of dilute BEC is absolutely justified. Our numerical analysis also verifies its truth as the correlation function properly reproduces the dimer wave function. Thus our correlated many-body calculation offers a good testing ground for the shape-independent approximation and for the correlation properties for a wide range of particle numbers. The first part of our work considers the dilute and weakly interacting regime, when the diluteness condition $n|a_s|^3 \ll 1$ is valid, with n being the number density of atoms in the trap. The comparison with the mean-field and Thomas-Fermi results at large particle number will exhibit the role played by the shape-dependent two-body interaction potential even in the extreme dilute condition.

In present-day experiments, a magnetic field under proper condition is used to tune the interatomic potential and a physically dilute but strongly interacting condensate is produced near the Feshbach resonance [6–8]. Thus in the second part of our work, we are interested to push our correlated basis functions for dilute ($n|a_s|^3 < 1$) but large scattering lengths. The natural ^{87}Rb scattering length is $100a_0$, with a_0 being the Bohr radius. We also choose a few other scattering lengths, viz. $200a_0$, $400a_0$, $600a_0$, $800a_0$, and $1000a_0$, for the same system of A trapped atoms. In this regime, the shape-independent approximation fails and the mean-field theory becomes measurably bad. We observe strong dependence of the correlation energy, both on the number of atoms and on the scattering length. This definitely shows the importance of many-body physics beyond the mean-field approach. The calculated

*Permanent address: Nuclear Division, Aveng Africa Limited, 204 Rivonia Road, Morningside 2057, South Africa.

 ©2013 American Physical Society

one-body density also shows very strong dependence on both the particle number and the scattering length. The one-body aspects of zero-temperature BEC reveals the finite-size effect where the quantum fluctuation is very important.

The paper is organized as follows. In Sec. II, we briefly describe the correlated potential harmonic basis and the technique to push it for particle numbers of the order of millions. In Sec. III, we present our numerical procedure and the results. In Sec. IV, we draw our conclusions.

II. METHODOLOGY

A. Correlated potential harmonic basis

The Schrödinger equation for a system of $A = N + 1$ identical bosons of mass m, confined by an externally applied trapping potential $V_{\rm trap}$ and interacting via a two-body potential $V(\vec{r}_i - \vec{r}_j)$, is

$$\left[-\frac{\hbar^2}{2m} \sum_{i=1}^{A} \nabla_i^2 + \sum_{i=1}^{A} V_{\rm trap}(\vec{r}_i) + \sum_{i,j>i}^{A} V(\vec{r}_i - \vec{r}_j) - E \right] \Psi(\vec{r}_1, \ldots, \vec{r}_A) = 0, \quad (1)$$

where E is the total energy of the system and $\vec{r}_i$ is the position vector of the ith particle. Introducing N Jacobi vectors $(\vec{\zeta}_i,\ i = 1, \ldots, N)$, the center-of-mass motion is separated and the relative motion is described by

$$\left[-\frac{\hbar^2}{m} \sum_{i=1}^{N} \nabla_{\zeta_i}^2 + V_{\rm trap} + V_{\rm int}(\vec{\zeta}_1, \ldots, \vec{\zeta}_N) - E_R \right] \Psi(\vec{\zeta}_1, \ldots, \vec{\zeta}_N) = 0, \quad (2)$$

where $V_{\rm int}$ is the sum of all pairwise interactions. E_R is the relative energy of the system, i.e., $E = E_R + 3/2\hbar\omega$, where ω is the trap frequency. We choose the relative separation $\vec{r}_{ij}$ of the (ij)-interacting pair as $\vec{\zeta}_N$, whose polar coordinates are (ϑ, φ), and define the hyperradius (r) of the set of A particles as $r^2 = \sum_{i=1}^{N} \zeta_i^2$. Next, introducing the hyperangles (Ω_N) as in Ref. [9], the Schrödinger equation for the relative motion is expressed in terms of the hyperspherical variables. In the hyperspherical harmonic expansion method (HHEM) [9], the relative wave function is expanded in the complete set of hyperspherical harmonics (HH), which are a $3N$-dimensional generalization of spherical harmonics. The HH basis keeps all possible correlations. However, as already mentioned, due to large degeneracy in the HH basis, which increases very rapidly with A, the HHEM becomes impractical for $A > 3$. For dilute BEC, *only* two-body correlations are important, as the possibility of depletion of the condensate due to three-body recombination is negligible. Thus, instead of choosing the full HH basis, we can choose a subset, called the potential harmonics (PH) subset [10,11], which involves two-body correlations only. The PH basis was introduced by Fabre long ago to treat nuclear systems, where disregard of higher-body correlations was doubtful. However, in the context of dilute BEC, the choice of two-body correlation is meaningful and the PH basis set may be a good correlated basis set for the description of various properties of the dilute BEC. It implies that when an (ij) pair interacts, the remaining particles are noninteracting spectators. This picture is true for all possible (ij) pairs. We define the hyperradius for the $(N-1)$ noninteracting particles as $\rho_{ij}^2 = \sum_{i=1}^{N-1} \zeta_i^2$, so that $r^2 = \rho_{ij}^2 + r_{ij}^2$, since $\vec{r}_{ij} = \vec{\zeta}_N$. Then, the hyperangle ϕ is introduced such that $r_{ij} = r\ \cos\phi$ and $\rho_{ij} = r\ \sin\phi$. The BEC many-body wave function Ψ is then written as a sum of two-body Faddeev components $\Psi = \sum_{i,j>i}^{A} \phi_{ij}$, where $\phi_{ij} = \phi_{ij}(\vec{r}_{ij}, r)$. Since only two-body correlations are relevant, the Faddeev component ϕ_{ij} is independent of the coordinates of all the particles other than the interacting pair. Thus the angular and hyperangular momenta for the (ij) partition of the system are contributed by the interacting pair only. ϕ_{ij} is then expanded in the PH basis $\{\mathcal{P}^{\ell m}_{2K+\ell}(\Omega_N^{ij})\}$, which is the subset of HH necessary for the expansion of $V(\vec{r}_{ij})$, as

$$\phi_{ij} = r^{-(3N-1)/2} \sum_{K} \mathcal{P}^{lm}_{2K+l}(\Omega_N^{ij}) u^l_K(r). \quad (3)$$

Note that $\{\mathcal{P}^{\ell m}_{2K+\ell}(\Omega_N^{ij})\}$ depends only on $\vec{r}_{ij}$, i.e., $\vec{\zeta}_N$, and is independent of $(\vec{\zeta}_1, \ldots, \vec{\zeta}_{N-1})$, and $\Omega_N^{(ij)}$ denotes the full set of hyperangles in $3N$-dimensional space for the choice $\vec{\zeta}_N = \vec{r}_{ij}$. Substitution of this in the Faddeev equation for the (ij) partition and projection on the PH corresponding to the (ij) partition gives a set of coupled differential equations (CDE),

$$\left\{ -\frac{\hbar^2}{m}\frac{d^2}{dr^2} + \frac{\hbar^2[\mathcal{L}(\mathcal{L}+1) + 4K(K+\alpha+\beta+1)]}{mr^2} - E_R + V_{\rm trap}(r) \right\} U_{K\ell}(r) + \sum_{K'} \overline{V}_{KK'}(r) U_{K'\ell}(r) = 0, \quad (4)$$

where $\overline{V}_{K,K'}(r) = f_{K\ell} V_{KK'}(r) f_{K'\ell}$, $U_{K\ell}(r) = f_{K\ell} u^{\ell}_K(r)$, $\mathcal{L} = \ell + (3A-6)/2$, $\alpha = (3A-8)/2$, and $\beta = \ell + 1/2$, with ℓ being the orbital angular momentum contributed by the interacting pair; $f^2_{K\ell}$ is a constant representing the overlap of the PH for interacting partition with the sum of PHs of all partitions [10], while $V_{KK'}(r)$ is the potential matrix element [11] and is given by

$$V_{KK'}(r) = \int P^{lm^*}_{2K+l}(\Omega_N^{ij}) V(r_{ij}) P^{lm}_{2K'+1}(\Omega_N^{ij}) d\Omega_N^{ij}. \quad (5)$$

One can, in principle, solve Eq. (4) exactly or by adiabatic approximation to obtain the energy and wave function of the condensate.

B. Short-range correlation for a finite-range potential

In the dilute laboratory BEC, the average interparticle separation is much larger than the actual range of the two-body interatomic interaction, irrespective of the numerical value of a_s. This is indeed necessary to prevent molecule formation via three-body recombination and external depletion of the condensate. Due to this and also the fact that the energy of the interacting pair is negligibly small compared to the energy scale of the interatomic interaction, the *effective two-body interaction* is characterized by the zero-energy scattering. Thus the effective interaction is described by the s-wave scattering length a_s. However, this is strictly true only for small $|a_s|$ in

the low-density regime, $n|a_s|^3 \ll 1$, with n being the number density. The assumption of a zero-range contact interaction makes its strength proportional to a_s. This assumption in the mean-field theory gives rise to the GP equation. Thus, for positive a_s, the condensate is called repulsive, whereas negative a_s corresponds to the attractive condensate. Hence, the GP equation presents a good description in the low-density limit. But, for larger $|a_s|$, for which $n|a_s|^3$ becomes comparable with 1, the two-body interaction strength depends on the energy scales involved and is no more proportional to a_s. Thus for larger values of $|a_s|$, the GP equation is less reliable. For intermediate values, the Lee-Huang-Yang (LHY) correction [12] accounts for the deviations. For very large values of a_s close to the Feshbach resonance, the GP equation breaks down. Besides this, the finite range of the realistic two-body interaction introduces corrections, which are shape dependent and not universal. Uniform condensates of dense Bose gases, having large positive a_s and interacting through an attractive short-range interaction, were studied by Cowell *et al.* [13] and by Song and Zhou [14]. It was observed that the mean-field result including the LHY correction differs greatly from the more exact calculations. Furthermore, the energy per particle, chemical potential, etc. approach a saturation value as a_s increases beyond the average interparticle separation. It was also observed that the energy of the Bose gas is related to that of the Fermi gas near the Feshbach resonance. These results are strikingly different from those using the GP equation.

Thus it is interesting to study the behavior of trapped Bose gases approaching the Feshbach resonance by an *ab initio* approach. Inclusion of a finite-range realistic two-body interaction is also important. Note that a realistic interatomic interaction is always attractive at larger separations, and has a strong short-range repulsion. The latter produces a short-range correlation that forbids the interacting pair to come too close together. To account for the strong repulsion between the bosons at short separations, we include an additional short-range correlation function $\eta(r_{ij})$ in the expansion of ϕ_{ij} [15]. This $\eta(r_{ij})$ is obtained as the zero-energy solution of the two-body Schrödinger equation with $V(r_{ij})$,

$$\left[-\frac{\hbar^2}{m}\frac{1}{r_{ij}^2}\frac{d}{dr_{ij}}\left(r_{ij}^2\frac{d}{dr_{ij}}\right)+V(r_{ij})\right]\eta(r_{ij})=0. \tag{6}$$

Its asymptotic form quickly attains $\eta(r_{ij}) \sim C(1-a_s/r_{ij})$, from which a_s is obtained [16]. In our earlier calculation [15], we have verified that $\eta(r_{ij})$ correctly reproduces the dimer wave function. Inclusion of $\eta(r_{ij})$ in the PH basis dramatically enhances the rate of convergence of the expansion (since it correctly follows the short-separation behavior), but at the same time it makes the expansion basis nonorthogonal. Standard procedure can handle this, but the process becomes quite involved and slow in the numerical procedure. Actual calculation shows that $\eta(r_{ij})$ is different from a constant only in a very narrow interval near the origin, in the BEC length scale. This makes the overlap matrix close to a constant matrix. Its effect is then approximately taken through the empirically obtained asymptotic constant C. The corresponding correlated potential matrix element is given by [15]

$$V_{KK'}(r)=\frac{1}{\sqrt{\left[h_K^{\alpha,\beta}h_{K'}^{\alpha,\beta}\right]}}\int_{-1}^{+1}P_K^{\alpha,\beta}(z)V[r\sqrt{(1+z)/2}] \times P_{K'}^{\alpha,\beta}(z)\eta[r\sqrt{(1+z)/2}]W_\ell(z)dz. \tag{7}$$

Here $h_K^{\alpha,\beta}$ and $W_\ell(z)$ are, respectively, the norm and weight function [17] of the Jacobi polynomial $P_K^{\alpha,\beta}(z)$. As a realistic interatomic potential, we choose the van der Waals potential. The short-range behavior is modeled by a hard core of radius r_c, which is adjusted to give experimental a_s [16]. For the hard-core potential, the lower limit of integration in Eq. (7) is replaced by $z_{\min}=2(\frac{r_c}{r})^2-1$.

We tested the correlated potential harmonic expansion (CPHE) method for both repulsive and attractive BECs: for attractive BEC, the experimental stability factor is very accurately reproduced compared to mean-field results, while properties of repulsive BECs have been extensively reproduced for $A \leqslant 15\,000$ [11,15,18–20]. Although these were in good agreement with other theoretical results obtained in that range, still the number of particles is quite far from the real experimental situation for repulsive BECs. Extending this for the $A \to \infty$ limit is a very challenging problem. There is no unique many-body calculation which can describe accurately the properties of interacting bosons for the entire range of atoms—from a few tens to several millions. For such a unique description, interatomic correlations and the realistic interatomic interaction are essential. CPHE may be an ideal starting point in this direction. In the CPHE approach used so far, the potential matrix involves integration containing Jacobi polynomial $P_K^{\alpha,\beta}(z)$ and its weight function $W_l(z)$. In the $A \to \infty$ limit, both of them change very rapidly with z, which generates severe numerical problems. With careful numerical handling [15], we pushed the CPHE limit to A = 15 000 atoms. This method for moderately large A is referred to as the CPHEM. However, for $A > 15\,000$, the calculation of $V_{KK'}(r)$ is already beyond the limit of a computer. It needs further theoretical analysis such that one can push the CPHE to the $A \to \infty$ limit.

C. Extension of CPHE to the $A \to \infty$ limit

In the present work, we utilize a mathematical transformation, employed in Refs. [21,22], to deal with the aforementioned problems. Within this transformation, the Jacobi polynomial $P_K^{\alpha,\beta}(z)$ transforms for large α (i.e., for large A) to the associated Laguerre polynomial $L_K^{\beta}(\zeta^2)$, where $\zeta^2=\alpha(1+z)/2$, in the limit $\alpha \to \infty$. In the same limit, the weight function of the Jacobi polynomial goes over to the weight function $\zeta^{2\beta}e^{-\zeta^2}$ of the associated Laguerre polynomial. Both are smooth functions of their arguments and thus the difficulties with the Jacobi polynomials can be bypassed. The potential matrix $V_{KK'}(r)$, in the transformed correlated potential harmonic expansion method for large number of particles (CPHEL), takes the form

$$V_{K,K'}(r)=A_c\int_{x_{\min}}^{\alpha}L_K^{\beta}(x)V\left(r\sqrt{\frac{x}{\alpha}}\right)\eta\left(r\sqrt{\frac{x}{\alpha}}\right) \times L_{K'}^{\beta}(x)x^{\beta}\exp(-x)dx, \tag{8}$$

where A_c is a constant given by

$$A_c = \frac{(-1)^{K+K'}}{\alpha^{\beta}} \left\{ \left(\frac{2K+\alpha+\beta+1}{\alpha} \right) \left(\frac{2K'+\alpha+\beta+1}{\alpha} \right) \times \left[\frac{\Gamma(K+1)}{\Gamma(K+\beta+1)} \right] \left[\frac{\Gamma(K'+1)}{\Gamma(K'+\beta+1)} \right] \times \left[\frac{\Gamma(K+\alpha+\beta+1)}{\Gamma(K+\alpha+1)} \frac{\Gamma(K'+\alpha+\beta+1)}{\Gamma(K'+\alpha+1)} \right] \right\}^{1/2}, \quad (9)$$

and $x_{\min} = (r_c/r)^2\alpha$, with r_c being the hard-core radius of our chosen realistic van der Waals potential.

III. NUMERICAL PROCEDURE AND RESULTS

A. Solution of coupled differential equation

Restricting the K sum in Eq. (3) to an upper limit of $K_{\max}$ (which is determined from the requirement of convergence), we solve the set of coupled differential equations (CDE) [Eq. (4)] by hyperspherical adiabatic approximation (HAA) [23]. Assuming that the hyperradial motion is slow compared to the hyperangular motion, the latter is separated adiabatically and solved for a fixed value of r. This is achieved by diagonalizing the potential matrix together with the hypercentrifugal repulsion for a fixed r. The lowest eigenvalue $\omega_0(r)$ gives the effective potential (as a parametric function of r) in which the condensate moves [11]. In the uncoupled adiabatic approximation (UAA), an overbinding correction term is also included with $\omega_0(r)$ [23]. Although Eq. (4) can be solved by an exact numerical algorithm, e.g., the renormalized Numerov method [24], we employ here the extreme adiabatic approximation, neglecting the overbinding correction term of the UAA. Thus in HAA, the approximate solution (the energy and wave function) of the condensate is obtained by solving a single uncoupled differential

TABLE I. Calculated minimum of eigenpotential ($\omega_0|_{\min}$), its position, and excitation energies of the two lowest l states (E_{01} and E_{02}) (all in o.u.) and the CPU time for different $K_{\max}$ values and different A. This table shows the extremely fast convergence of the correlated PH basis expansion.

A	$K_{\max}$ Quantity	2	4	6
100	$\omega_0\|_{\min}$	165.251233	165.249242	165.248840
	at	18.53	18.53	18.53
	E_{01}	2.0542	2.0542	2.0542
	E_{02}	4.1082	4.1082	4.1082
	CPU time (h:m:s)	0:13:17	0:39:51	1:21:38
1000	$\omega_0\|_{\min}$	2431.556579	2431.549665	2431.549300
	at	74.22	74.22	74.22
	E_{01}	2.1685	2.1685	2.1685
	E_{02}	4.3369	4.3369	4.3369
	CPU time (h:m:s)	0:16:35	0:49:46	1:41:58
10000	$\omega_0\|_{\min}$	51986.15544	51986.07882	51986.07505
	at	351.16	351.15	351.15
	E_{01}	2.2228	2.2229	2.2228
	E_{02}	4.4456	4.4455	4.4456
	CPU time (h:m:s)	0:18:22	0:55:06	1:52:51
20000	$\omega_0\|_{\min}$	135140.95468	135140.73302	135140.71626
	at	567.54	567.54	567.54
	E_{01}	2.2283	2.2283	2.2283
	E_{02}	4.4566	4.4566	4.4565
	CPU time (h:m:s)	0:17:08	0:51:27	1:45:24
100000	$\omega_0\|_{\min}$	1267040.91207	1267040.48387	1267040.45244
	at	1742.12	1742.12	1742.12
	E_{01}	2.2339	2.2339	2.2339
	E_{02}	4.4678	4.4678	4.4678
	CPU time (h:m:s)	0:19:23	0:58:11	1:59:10
1000000	$\omega_0\|_{\min}$	31670143.0254	31670141.9141	31670141.8652
	at	8716.92	8716.92	8716.92
	E_{01}	2.2357	2.2357	2.2358
	E_{02}	4.4714	4.4714	4.4715
	CPU time (h:m:s)	0:28:42	1:26:06	2:56:20

equation,

$$\left[-\frac{\hbar^2}{m}\frac{d^2}{dr^2}+\omega_0(r)-E_R\right]\zeta_0(r)=0, \tag{10}$$

subject to appropriate boundary conditions on $\zeta_0(r)$. The function $\zeta_0(r)$ is the collective wave function of the condensate in the hyperradial space. The lowest-lying state in the effective potential $\omega_0(r)$ corresponds to the ground state of the condensate. The total energy of the condensate is obtained by adding the energy of the center-of-mass motion ($\frac{3}{2}\hbar\omega$) to E_R. The advantages of this approach are as follows: first, the HAA basically reduces the $3N$-dimensional problem to an effective one-dimensional one, where the lowest eigenpotential exhibits all necessary features of BEC; second, the PH basis includes the two-body correlations exactly and yet the number of variables involved is *only four* for any A; third, the use of a realistic (van der Waals) potential takes both the short-range repulsion and long-range correlation correctly into account and finally, one is, basically, facing the task of solving a system of coupled, single-variable, differential equations of limited small rank for any A.

B. Results

We use oscillator units (o.u.) throughout, in which length and energy are expressed in the units of $a_{ho}=\sqrt{\hbar/m\omega}$ and $\hbar\omega$, respectively. We have already mentioned that the interatomic potential is chosen as the van der Waals potential with a hard core of radius r_c, viz. $V(r_{ij})=\infty$ for $r_{ij}\leqslant r_c$, and $=-\frac{C_6}{r_{ij}^6}$ for $r_{ij}>r_c$. The strong short-range repulsion is parameterized by the hard core and the strength (C_6) is known for a given type of atom, e.g., $C_6=6.4898\times10^{-11}$ o.u. for Rb atoms [16]. The value of r_c is adjusted to get the desired value of a_s [16].

First we check the rate of convergence of the correlated PH basis expansion as the maximum value of grand orbital quantum number $K_{\max}$ increases. In Table I, we present calculated values of the minimum of eigenpotential ($\omega_0|_{\min}$), its position (both in o.u.), excitation energies of the first two $l=0$ excited states (E_{01} and E_{02}) in o.u., and the CPU time (on a Dell Inspiron Core2 Duo laptop computer) for different $K_{\max}$ values and different particle number (A). We notice that the rate of convergence as $K_{\max}$ increases is extremely fast, particularly as $K_{\max}$ or A increases. For example, for $A=10\,000$, $\omega_0|_{\min}$ changes by only about $7.3\times10^{-6}\%$ as $K_{\max}$ increases from 4 to 6. The change becomes smaller as either $K_{\max}$ or A increases. For $A=10^6$, the percentage change between $K_{\max}=4$ to $K_{\max}=6$ is about 1.5×10^{-7}. Other calculated quantities remain practically unchanged. This extremely fast convergence is due to the use of our correlated PH basis, which correctly simulates the very short-range behavior of the interacting-pair Faddeev component. We checked that the rate of convergence of an uncorrelated PH basis expansion is much slower. This emphasizes the very important role played by our correlated PH basis. On the other hand, the CPU time increases quickly with $K_{\max}$, and to a smaller extent with A. Hence we restrict the K values to a $K_{\max}=4$. For $A>15\,000$, CPHEL is used. Thus $A=10\,000$ and $A=20\,000$ are calculated using CPHEM and CPHEL, respectively. One can notice that the CPU time needed for the same $K_{\max}$ is smaller for $A=20\,000$ than that needed for $A=10\,000$, in spite of an increase of A by a factor of two. This shows that the CPHEL is faster than the CPHEM.

TABLE II. Ground-state energy per particle (in o.u.) obtained by CPHEM for different number (A) of ^{87}Rb atoms in the condensate for two choices of $a_s=100$ and 1000 Bohr. DMC results are also presented for comparison [3].

a_{sc}	A	CPHEM	DMC
100	3	1.512	1.503
	5	1.511	1.507
	10	1.523	1.515
	20	1.548	1.532
	100	1.677	1.651
1000	3	1.549	1.534
	5	1.595	1.567
	10	1.713	1.642
	20	1.890	1.773
	50	2.158	2.079
	100	2.534	2.454

For the next part of our work, we consider the BEC experiment at the JILA trap for which $a_s=100$ Bohr $=0.00433$ o.u. [1]. The ground-state energy per particle obtained by our CPHEM for few particles is presented in Table II.

We also present available results of DMC for comparison. The nice agreement with our correlated but approximate many-body approach and the exact many-body calculation demonstrates the importance of correlation in the two-particle level for dilute and weakly interacting BEC. Due to the computational difficulty, DMC results are available only up to ∼100 atoms. However, we can run our many-body code for quite a large number of atoms (∼millions) without any computational difficulty. This is because of the fact that the total number of active degrees of freedom remains always *four*, irrespective of the number of atoms. For further comparison with large atom number, we plot the energy per atom in Fig. 1.

GP and Thomas-Fermi (TF) model results are also presented. TF results are always lower than both the GP and

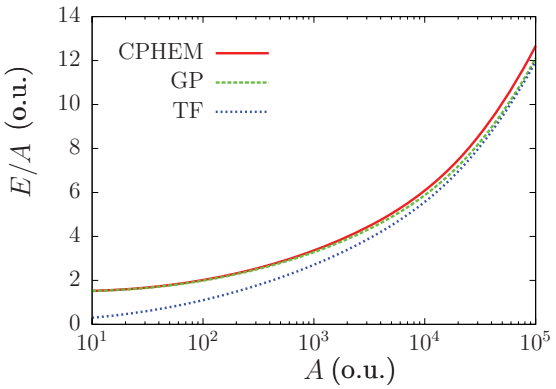

FIG. 1. (Color online) Ground-state energy per atom (in o.u.) by the correlated potential harmonics expansion approach as a function of the number of bosons A (using log scale) in the condensate of ^{87}Rb atoms with $a_s=100$ Bohr. GP and TF results are also shown for comparison.

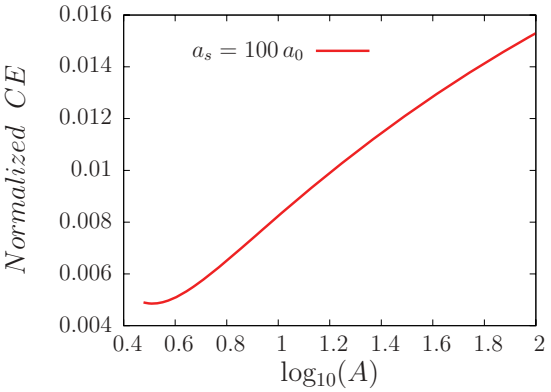

FIG. 2. (Color online) Normalized correlation energy as a function of $\log_{10}(A)$ in the condensate of ^{87}Rb atoms with $a_s = 100$ Bohr.

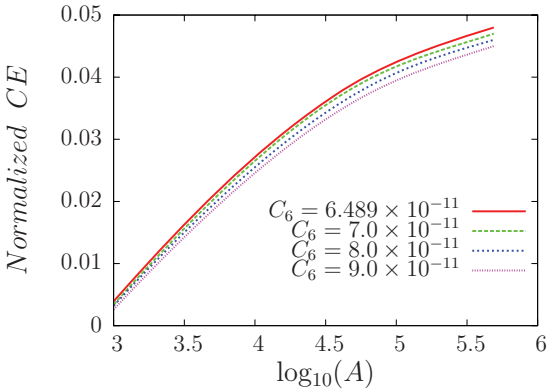

FIG. 3. (Color online) Normalized correlation energy as a function of $\log_{10}(A)$ in the condensate of ^{87}Rb atoms with $a_s = 100$ Bohr and different choices of C_6 parameter.

many-body results, as the kinetic-energy term is completely ignored in the TF limit. However, the difference between many-body and mean-field energies exists both for moderate and large numbers of atoms. It indicates that even for such small scattering lengths, interatomic correlation plays an important role. We refer to the energy difference $E_{\text{many-body}} - E_{GP}$ as a correlation energy (E_{CE}).

Normalized correlation energy is defined as $\frac{E_{CE}}{E_{\text{many-body}}}$ and has been shown as a function of $\log_{10}(A)$ in Fig. 2. Correlation energy smoothly increases with particle number, which clearly shows the presence of particle-particle correlation.

Besides the limitation of the GP theory arising from the assumption of a constant strength of the effective interaction, its use of a shape-independent zero-range potential for the interatomic interaction needs to be examined. To test the validity of this shape-independent approximation (SIA), we calculate correlation energy as before by gradually increasing C_6, keeping a_s unchanged.

The hard-core radius is appropriately changed to get the same $a_s = 100$ Bohr [16]. With an increase in C_6, the strength of the long-range attractive interaction increases, which causes an increase in the actual two-body attraction $[4\pi \int_{r_c}^{\infty} V(r) r^2 dr]$. The net many-body energy thus decreases and the correlation energy also decreases with an increase in the C_6 parameter, as shown in Fig. 3. Thus our many-body calculation acts as the test bed for the validity of the SIA and to study many-body physics beyond the mean-field approach.

As already stated in Sec. I, the second important motivation of our present study is to push the correlated basis function for larger scattering lengths. In the present work, we limit a_s up to 1000 Bohr and study several ground-state properties. We also show how the effect of correlation gradually builds in with a continuous increase in scattering length. Thus this part of our work considers still dilute, but strongly interacting BEC, where the use of the two-body correlated basis function is fairly justified. In this limit, mean-field theory and the shape-independent approximation break down and the beyond-mean-field effects come into the picture. In Table II, we also present both the many-body and DMC energies for up to 100 particles with $a_s = 1000$ Bohr.

Although the DMC and CPHEM results are in close agreement, many-body energy is slightly but consistently higher than the DMC results. It may be noted that the DMC calculation used purely repulsive hard-core potential or the sum of repulsive and attractive Gaussians, whereas our many-body theory used the hard core with a long-range attractive tail. It may be because the shape-dependent potential plays an important role for larger scattering lengths. In Fig. 4, we plot the condensate energy per atom as a function of particle number for $a_s = 1000$ Bohr. In the same figure, GP results are also presented. The large deviation between the mean-field and many-body energy even for a few-thousand particles shows that the mean-field approximation is no longer accurate in such density regime. The interatomic correlation also plays a significant role here. In Fig. 4, we restricted A up to 10 000. It should be noted that we can obtain results for $A > 10\,000$, but the mean-field results become unstable in this limit.

Next, to quantify the effect of correlation, we gradually tune the scattering length from 100 to 1000 Bohr. We calculate the normalized correlation energy as before and plot it in Fig. 5 as a function of scattering length for a fixed number of particles in the trap. We observe that correlation energy smoothly increases with a_s for $A = 1000$. In this particle limit, the finite-size effect also comes in, which is beyond the scope of study in the mean-field approach. For $A = 10\,000$, the normalized correlation

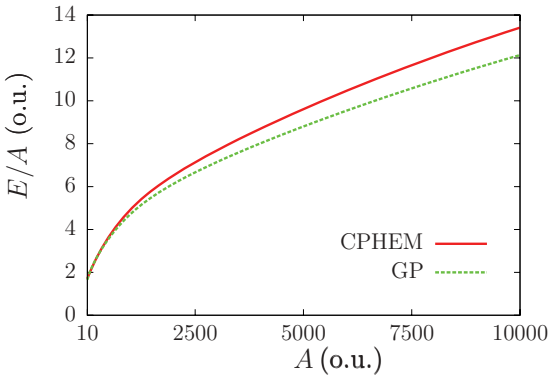

FIG. 4. (Color online) Ground-state energy per atom (in o.u.) as a function of the number of bosons A in the condensate of ^{87}Rb atoms with $a_s = 1000$ Bohr. GP energy is also presented for comparison.

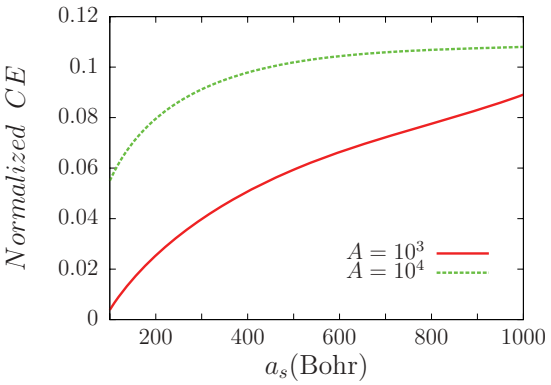

FIG. 5. (Color online) Normalized correlation energy as a function of scattering length for indicated fixed number of atoms in the condensate.

energy is large; however, with an increase in scattering length, it gradually saturates. It indicates that with a further increase in a_s, the normalized correlation energy does not change. Thus the condensate will exhibit the universal behavior of saturation in relative correlation energy when the scattering length will be the order of the trap size.

The other important aspect of our present study is the ground-state correlation properties with various scattering lengths. We are especially interested in the one-body density, which contains information regarding the one-particle aspect of the bosonic system. Although it is not directly measurable, one can indirectly explore it in the interferometry experiments. We define the one-body density as the probability density of finding a particle at a distance $\vec{r}_k$ from the center of mass of the condensate as

$$R_1(\vec{r}_k) = \int_{\tau'} |\Psi|^2 d\tau', \tag{11}$$

where Ψ is the full many-body wave function and the integral over the hypervolume τ' excludes the variable $\vec{r}_k$. After a lengthy but straightforward calculation, we arrive at a closed form given by

$$R_1(\vec{r}_k) = \frac{2^{\alpha+1/2}}{\pi^{3/2}} \int_0^\infty \int_{-1}^1 \left[\frac{\Gamma((D-3)/2)}{\Gamma((D-6)/2)}\right] [\zeta_0(r')]^2 \times \sum_{KK'} \frac{\chi_{K0}(r')\chi_{K'0}(r')}{f_{Kl} f_{K'l}} \frac{P_K^{\alpha\beta}(z) P_{K'}^{\alpha\beta}(z)}{\left[h_K^{\alpha\beta} h_{K'}^{\alpha\beta}\right]^{1/2}} \times \sqrt{\frac{1+z}{2}} \left(\frac{1-z}{2}\right)^{(D-8)/2} \times \left(r'^2 + 2r_k^2\right)^{(1-D)/2} r'^{D-4} dr' dz, \tag{12}$$

where $D = 3A - 3$ and $h_K^{\alpha\beta}$ is the norm of the Jacobi polynomial $P_K^{\alpha\beta}(z)$. In Fig. 6, we present calculated one-body density as a function of the distance from the trap center for $A = 10\,000$ with various a_s. The effect of the interaction is revealed by the deviation from the Gaussian profile. We observe sharp changes in $R_1(\vec{r}_k)$ as a_s increases. For $a_s = 100$ Bohr, the density distribution is sharper as the correlation induced by the interaction is weak, while for $a_s = 1000$ Bohr, the peak is flatter with a large width.

The important point to be noted is that our correlated many-body approach takes care of the effect of finite size, where quantum fluctuation is important. To observe the effect of finite size, we calculate the one-body density for fixed effective interaction Aa_s and plot it in Fig. 7. In the mean-field theory, the net interaction is determined by the effective interaction parameter (Aa_s) and does not take into account the finite-size effect, whereas the many-body results strongly depend on A and a_s separately. In Fig. 7, we observe that the many-body graphs separate for $A = 1000$ and $A = 10\,000$ for the same Aa_s. Thus in the finite-particle range, where the effect of quantum fluctuation is important, our many-body result strongly deviates from the mean-field result and gives the realistic picture of correlation properties.

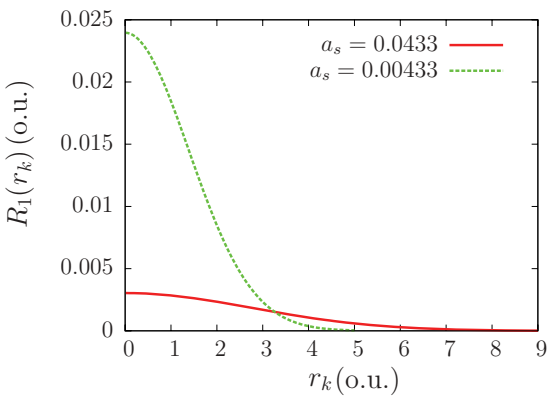

FIG. 6. (Color online) One-body density distribution as a function of r_k (in o.u.) for ^{87}Rb atoms in the condensate with $A = 10\,000$ bosons. Plots shown are for $a_s = 100$ Bohr (0.00433 o.u., green dashed line) and 1000 Bohr (0.0433 o.u., red solid line).

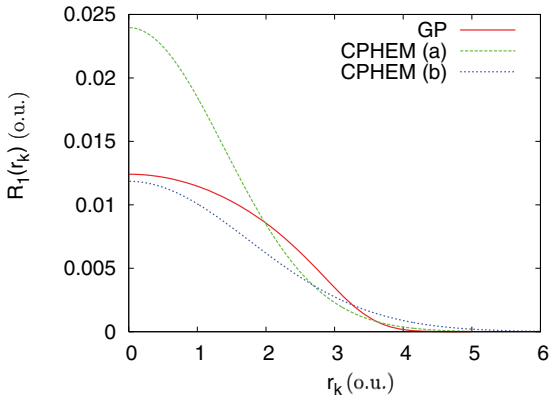

FIG. 7. (Color online) One-body density distribution as a function of r_k (in o.u.) for ^{87}Rb atoms in the condensate for fixed effective interaction $Aa_s = 43.3$ (in o.u.). The (a) GP and CPHEM results are for $A = 10\,000$, $a_s = .00433$ o.u. and (b) CPHEM for $A = 1000$, $a_s = .0433$ o.u.

IV. CONCLUSION

This paper presents an approximate quantum many-body calculation for the inhomogeneous Bose gas. It uses the van der Waals interaction and keeps all possible two-body correlations. This two-body correlated basis function is successfully applied for any number of bosons in the dilute weakly interacting Bose gas. Our quantum many-body calculation can handle the entire range of particles which is experimentally achieved, and thus our many-body theory basically serves as a stringent test of the mean-field theory for the entire range of particles. It is also used as the *testing bed* for the validity of the shape-independent approximation (SIA). In the study of ground-state properties, we observe the breakdown of SIA, as the interatomic correlation plays an important role even in the dilute regime. Next we push the correlated basis function for larger scattering lengths, while the condensate is still dilute, such that the two-body collisions only remain significant. Thus our many-body theory provides a *bottom-up* research to give the realistic picture of the ground-state properties. For large scattering lengths, we observe a noticeable breakdown in the mean-field results and the correlation energy shows saturation properties in the limit of large particle numbers. The calculation of one-body density also highlights the one-particle aspect of the bosonic system. We also observe the finite-size effect in the one-body densities.

The present study is limited to dilute systems with large scattering lengths, but the condition $n|a_s|^3 < 1$ is still valid. In the future, it will be interesting to extend these studies for strongly interacting systems, where $n|a_s|^3$ is greater than 1, and see how far our correlated basis function will be appropriate to describe the properties of such BECs. The particularly interesting part will be the study of correlation properties near the Feshbach resonance where the condensate becomes highly correlated.

ACKNOWLEDGMENTS

T.K.D. and B.C. would like to thank the University of South Africa (UNISA) for their financial support of our visit to UNISA, where part of the work was done. B.C. also acknowledges financial support of DAE (India) under research Grant No. 2009/37/23/BRNS/1903.

[1] M. H. Anderson *et al.*, Science **269**, 198 (1995).
[2] F. Dalfovo, S. Giorgini, L. P. Pitaevskii, and S. Stringari, Rev. Mod. Phys. **71**, 463 (1999).
[3] D. Blume and C. H. Greene, Phys. Rev. A **63**, 063601 (2001).
[4] A. I. Streltsov, O. E. Alon, and L. S. Cederbaum, Phys. Rev. A **73**, 063626 (2006).
[5] I. Bloch, J. Dalibard, and W. Zwerger, Rev. Mod. Phys. **80**, 885 (2008).
[6] J. L. Roberts, N. R. Claussen, S. L. Cornish, E. A. Donley, E. A. Cornell, and C. E. Wieman, Phys. Rev. Lett. **86**, 4211 (2001).
[7] E. A. Donley *et al.*, Nature (London) **412**, 295 (2001).
[8] S. B. Papp, J. M. Pino, R. J. Wild, S. Ronen, C. E. Wieman, D. S. Jin, and E. A. Cornell, Phys. Rev. Lett. **101**, 135301 (2008).
[9] J. L. Ballot and M. Fabre de la Ripelle, Ann. Phys. (NY) **127**, 62 (1980).
[10] M. Fabre de la Ripelle, Ann. Phys. (NY) **147**, 281 (1983).
[11] T. K. Das and B. Chakrabarti, Phys. Rev. A **70**, 063601 (2004).
[12] T. D. Lee and C. N. Yang, Phys. Rev. **105**, 1119 (1957); T. D. Lee, K. Huang, and C. N. Yang, *ibid.* **106**, 1135 (1957).
[13] S. Cowell, H. Heiselberg, I. E. Mazets, J. Morales, V. R. Pandharipande, and C. J. Pethick, Phys. Rev. Lett. **88**, 210403 (2002).
[14] J. L. Song and F. Zhou, Phys. Rev. Lett. **103**, 025302 (2009).
[15] T. K. Das, S. Canuto, A. Kundu, and B. Chakrabarti, Phys. Rev. A **75**, 042705 (2007); T. K. Das, A. Kundu, S. Canuto, and B. Chakrabarti, Phys. Lett. A **373**, 258 (2009).
[16] C. J. Pethick and H. Smith, *Bose-Einstein Condensation in Dilute Gases* (Cambridge University Press, Cambridge, UK, 2002).
[17] *Handbook of Mathematical Functions*, edited by M. Abramowitz and I. A. Stegun (Dover, New York, 1964).
[18] A. Kundu, B. Chakrabarti, T. K. Das, and S. Canuto, J. Phys. B **40**, 2225 (2007).
[19] A. Biswas and T. K. Das, J. Phys. B **41**, 231001 (2008).
[20] B. Chakrabarti, T. K. Das, and P. K. Debnath, Phys. Rev. A **79**, 053629 (2009); A. Biswas, J. Phys. B **42**, 215302 (2009); A. Biswas, B. Chakrabarti, and T. K. Das, J. Chem. Phys. **133**, 104502 (2010); S. K. Haldar, B. Chakrabarti, and T. K. Das, Phys. Rev. A **82**, 043616 (2010); A. Biswas, T. K. Das, L. Salasnich, and B. Chakrabarti, *ibid.* **82**, 043607 (2010); P. K. Debnath and B. Chakrabarti, *ibid.* **82**, 043614 (2010); A. Biswas, B. Chakrabarti, T. K. Das, and L. Salasnich, *ibid.* **84**, 043631 (2011).
[21] R. M. Adam and S. A. Sofianos, Phys. Rev. A **82**, 053635 (2010).
[22] S. A. Sofianos, R. M. Adam, and V. B. Belyaev, Phys. Rev. C **84**, 064304 (2011).
[23] T. K. Das, H. T. Coelho, and M. Fabre de la Ripelle, Phys. Rev. C **26**, 2281 (1982).
[24] B. R. Johnson, J. Chem. Phys. **69**, 4678 (1978).